UNIVERSITY OF TEXAS AT ARLINGTON

MASTERS THESIS

An Integrated Design Tool for Tow-steered Composite Laminate in Abaqus

---

Author:
Twinkle Kothari

Supervisor:
Dr. Xin Liu

A thesis submitted in fulfillment of the requirements
for the degree of Masters of Science in Aerospace Engineering

at the

University of Texas at Arlington

December 2022

UNIVERSITY OF TEXAS AT ARLINGTON

Abstract

Masters of Science in Aerospace Engineering

An Integrated Design Tool for Tow-steered Composite Laminate in Abaqus

by Twinkle Kothari

The material of choice for contemporary aircraft and its component design over the past few decades has shifted more and more toward fiber-reinforced composites. This is mainly due to the improved strength, lightweight, corrosion resistance, design flexibility, and durability of composites over traditional metals. Advanced tailorable composites such as tow-steered composites can be designed and fabricated with fibers following prescribed curvilinear paths, which provides improved mechanical performance compared with unidirectional fiber-reinforced composites (UDFRCs). However, the potential of tow-steered composites oftentimes fails to be exploited due to the lack of design tools. Currently, there are no commercially available design tools for tow-steered composites and these advanced composite materials are often in off-optimal designs.

An integrated design tool for tow-steered composites is developed for commercial finite element (FE) software Abaqus via a graphical user interface (GUI) plug-in. This plug-in is written by Python scripts and incorporated all design definition setups so that users can design tow-steered composites in a unified environment within Abaqus. This design framework contains several components: design setups, multiscale plate modeling, FE structural analysis, and optimization. After the definition of design setups in the GUI plug-in, multiscale plate modeling is carried out by an external multiscale modeling code, which calculates the location-dependent shell stiffness matrix of each element in a FE model. The structural analysis with updated element properties can then be carried out by Abaqus. The optimization is performed by an external optimizer Dakota. The design variables are updated by Dakota and sent back to the FE model to compute structural responses to be employed in an objective function. Several examples are analyzed to demonstrate the use of the developed GUI plug-in.

This GUI plug-in provides a user-friendly and intuitive tool, which reduces the extra programming efforts of users so that they can focus on design innovations instead of code development. This work is supported through the Small Business Technology Transfer (STTR) program of the National Aeronautics and Space Administration (NASA).

Acknowledgements

I want to express my gratitude to my supervisor, Dr. Xin Liu, for his constant encouragement and motivation, as well as for his important guidance during my Masters. I would like to thank him for the helpful discussions and invaluable comments and to critically evaluate this manuscript.

I would like to thank my research advisors Dr Rassel Raihan and Dr Paul Davidson for their interest in my research and for taking the time to serve in my Thesis committee. I would like to thank Dr Kamesh Subbarao for his support as an advisor during my Masters.

I would also like to extend my appreciation to UTA and UTARI for providing financial support for my Masters. I would also like to thank NASA to financially support me during this period with their Small Business Technology Transfer (STTR) program.

I am grateful to all the teachers who taught me. I would also like to thank my colleagues with whom I worked with under the guidance of Dr Xin Liu.

Finally, I would like to express my deep gratitude to my parents who have encouraged me and sponsored my graduate studies. I am extremely grateful to them for their sacrifice, encouragement and patience. I would like to thank my sisters for encouraging and inspiring me to pursue graduate studies. I also want to thank some of my friends who have supported me all along the way.

Contents

List of Figures

List of Tables

Chapter 1

Introduction

1.1 Motivation

Improved high-performance structural materials are continually being developed as a result of the aerospace industry's unrelenting desire to increase the performance of military and commercial aircraft. Composites play a substantial role in both present-day and future aircraft components due to their exceptional strength/stiffness-to-weight ratios. Due to recent advances in fiber tow placement, tow-steered composite laminates result in fewer stress concentration zones and therefore offer improved mechanical properties with reduced weight. However, there are no commercial-grade software tools for the design optimization of tow-steered composites. Therefore, an integrated user-friendly design tool for tow-steered composites is urgently needed.

1.2 Literature review

1.2.1 Design of tow-steered composites

Composites are vastly used in aircraft structures as fuselage belly skins, ailerons, rudders, wings, and their components, etc. Tow-steered composites are used in rotorcraft fairings and rotor blades of helicopters to increase payload capacity and performance [1]. Space exploration mission components utilize lightweight structures for vehicles, solar arrays, antennas pressurized habitats, cryogenic tanks, landing

gears, and truss cages [2]. When compared to unidirectional fiber-reinforced composites (UDFRCs), tailorable composites provide great possibilities for further mass reduction and performance enhancement.

Guimaraes et al. used the classical lamination theory considering a symmetric stacking sequence and fiber trajectories described by Lagrange polynomials of different orders. The results are obtained for different optimization scenarios, aimed at increasing the flutter and linear buckling stability margins of tow-steered plates [3]. Jegley et al. demonstrated buckling, post-buckling, and failure behavior of elastically fitted panels using tape and tow-steered panels. The experimental findings depict the enhancements in buckling performance by utilizing tow-steered composites [4]. Wu et al. discussed the design and manufacturing of tow-steered composite shells for fuselage structures. Two cylindrical shells with tailored, tow-steered composites with varying fiber angle orientation were designed [5]. Stodieck et al. investigated the use of tow-steered composites to tailor the aeroelastic behavior of the composite wings. The effects on free vibration, flexural axis, flutter and divergence speeds, and gust loads were explored [6]. Stanford et al. exploited the benefits of tow-steered composite plates to improve static aeroelastic stresses and dynamic flutter boundaries [7]. Brooks et al. found reductions of up to 2.4% in fuel burn and 24% in wing weight when they used a combination of improved passive aeroelastic tailoring and local strength tailoring in high-stress regions in tow-steered structure for aero-structural wing design [8]. Barr and Jaworski explored the concept of passive tailoring to maximize power extraction from an NREL $5MW$ wind turbine blade. A 7% reduction in turbine power extraction at the rated wind speed and a 14% increase when the blade was tuned near the cut-in wind speed [9]. Singh and Kapania attempted to maximize the buckling load with a structural weight constraint for a two-layered composite laminate plate that is stiffened by four arbitrarily-placed stiffeners. The results showed that the arbitrarily-placed curvilinear stiffeners along the optimal curvilinear fiber paths in composite laminated skin can lead to more than 200% increase in the buckling load with weight reduction compared to UDFRCs [10]. All these previous works and applications point to the use of tow-steered composites for improved structural performance.

Unfortunately, for tow-steered composites, the capabilities of current design tools

lag behind the developing production techniques [11]. There are several drawbacks to the current design of tow-steered composites. The design tools frequently rely on glue language (like Python) to inter-operate between existing tools. These tools address the design variable setups, FE structural analysis, and optimization individually [12]. Particularly, when new design variables or material systems need to be taken into account, the design demands more programming work from the engineers [11]. Additionally, engineers are at better ease performing analysis using available professional FE tools (e.g., MSC. Patran/ Nastran and Dassault Systemes SIMULIA Abaqus). However, the current FE tools do not have integrated graphical user interfaces (GUI) to design tow-steered composites [11].

In addition to the limitations in the existing design tools, there are other limitations related to the theories that advocate the design. Most existing design tools are based on the classical lamination theory (CLT) and its improvements, which were initially created for UDFRCs. Structural behavior is often governed by semi-empirical rules derived from UDFRCs. The layup is restricted to quasi-isotropic stacking sequences and users treat composite materials as a "black aluminum" [11]. Even though certain novel theories have been created for modeling tow-steered composites, they still rely on predefined functions, such as the third-order shear deformation theory (TSDT) and zig-zag theories. Trinh et al. used a higher-order zig-zag displacement theory within the framework of the Hellinger-Reissner mixed variational principle for displacement prediction of tow-steered composites [13]. Groh et al. used the higher-order zig-zag theory to predict axial stress, lateral stress, in-plane shear stress, and transverse shear for laminates. The laminates include a variety of symmetric and non-symmetric, balanced and unbalanced, multi-material sandwich plates, as well as laminates with 3D heterogeneity [14]. Such assumptions unavoidably reduce the accuracy of structural behavior predictions and also restrict the development of the theory. Liguori et al. calculated deflection in variable stiffness composites that are subjected to large deformations. They use non-uniform rational basis spline (NURBS) interpolation codes to approximate the optimal distribution of lamination parameters using a gradient-based algorithm [12]. Though a p-version layer-wise approach is introduced for composite plates with curvilinear fibers to calculate plate stiffness by Yazdani and Ribeiro. The composite plate equations are in

the terms of ABD matrix [15].

In most structural analysis codes, the properties of shell elements can be input as the ABD matrix, while many newly developed theories do not have effective properties in terms of the ABD matrix. To include the non-standard shell element properties, special-purpose codes must be developed for these theories. As a result, the current design tools and theories cannot harness the full potential of tow-steered composites. In order to minimize assumptions and utilize the ABD matrix for shell elements, a more advanced multiscale plate modeling theory is required [11].

1.2.2 Mechanics of structure genome

The location-dependent properties of shell elements in a FE model are calculated using the mechanics of structure genome (MSG). The MSG uses structure genome (SG) as the smallest unit cell, which acts as the building block of structure. The MSG connects micromechanics and structural mechanics [11]. In Yu's model, for a one-dimensional (1D) beam continuum, the microstructure of each material point is a two-dimensional (2D) cross-section. The behavior of the 1D continuum is controlled by the 1D macroscopic beam analysis, but if the beam is additionally heterogeneous in the spanwise direction, a three-dimensional (3D) SG is required to compute effective beam stiffness for beam structural analysis. In plate-like structures without in-plane heterogeneity, like composite laminates, the SG is a 1D line segment along the thickness direction, with each segment designating each layer. The SG is 2D for a sandwich panel with a core that is corrugated in one dimension, and the SG is 3D for a heterogeneous panel in both in-plane directions. Every material point along a 2D continuum that represents a plate- or shell-like structure has the SG as its microstructure. This is depicted in Figure 1.1. In order to obtain the shell stiffness matrix for the macroscopic structural analysis, MSG homogenization is performed. After the macroscopic analysis, MSG performs dehomogenization to obtain the local fields (e.g. stress and strain) within the SG. Yu developed MSG and SwiftComp, a computer program that put the theory into practice [11]. To reduce information loss between homogenized and original models, the discrepancy between the strain energy density between homogenized and original models is minimized [16].

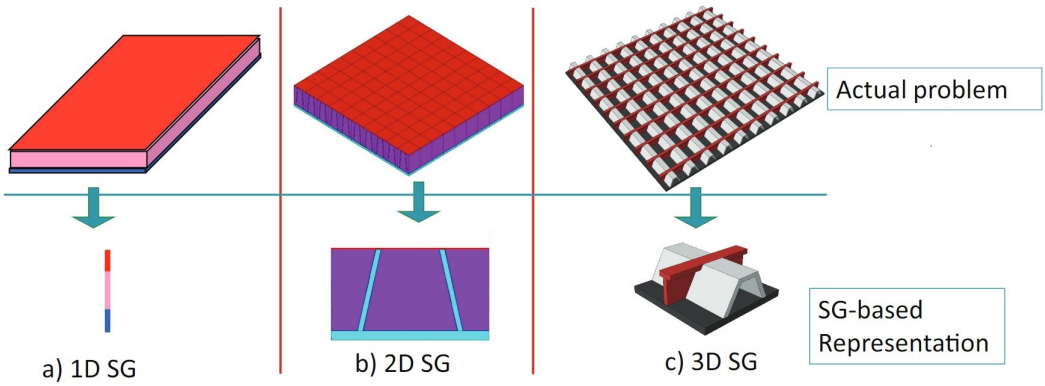

Figure 1.1: Plate-like structure vs corresponding constitutive SG (Source: Yu [11])

The MSG model has been applied to many multiscale plate modeling studies. Long and Yu constructed a plate model for variable stiffness laminates based on MSG [16]. Rouf et al. performed multiscale plate modeling of plate structures made of textile composites using MSG. The global displacement and local stress field results agreed well with the results from the direct numerical simulation. When compared to DNS, MSG-based analysis is substantially less expensive and requires less modeling work [17]. Liu et al. extended MSG to provide a unified approach to predict the thermo-elastic behaviors of composite structures. The accuracy of the structural responses and stress/ strain fields using the developed model was similar to that obtained from DNS [18]. Tao et al. used MSG-based modeling for printed circuit boards made of woven composites. It was noted that MSG analysis was much faster than the DNS [19]. Long et al. utilized microscale and mesoscale homogenization using MSG for analyzing a flat, thin flexure and lenticular composite boom in a simplified deployable structure. In the FE simulation of the column bending test, non-uniform deformation and stress from modified MSG agree well with Abaqus results [20]. Long et al. explored an MSG-based nonlinear shell model for a viscoelastic material. The generated model's analysis of a simple viscoelastic material and a continuum damage model both show excellent agreement with the DNS results [21].

In the MSG plate model, the idea is to reduce the discrepancy between the potential energy of the original 3D model and the equivalent plate model. Based on the

previous works, MSG consistently outperforms alternative models in terms of accuracy and efficiency. Therefore, the MSG model is an excellent choice for modeling advanced tow-steered composites.

1.3 Present work and outline

This work is supported by NASA to fully exploit the potential of tow-steered composites to improve space structures. The MSG is utilized for obtaining the effective properties of plate-like structures. An integrated design framework for tow-steered composites is developed as a graphical user interface (GUI) in FE software - Abaqus.

Chapter 2 contains the methodology of the MSG plate theory and the design framework.

Chapter 3 contains a detailed explanation of the main modules in the developed GUI plug-in.

Chapter 4 provides examples to illustrate the use of the designed GUI plug-in.

Chapter 5 concludes this thesis and points out future works.

Chapter 2

Methodology

2.1 MSG-based plate modeling

The MSG is a unified approach to multi-scale constitutive modeling of advanced materials and structures, which computes effective properties for the three-dimensional (3D) solids, plates/shells, and beams [22]. It contains all the material and geometrical information of a microstructure. The SG is a line segment with many connecting sub-line segments that represent a lamina. It is represented by 1D coordinates along the direction of the plate's thickness as shown in Figure 2.1a. The fluctuating functions w_i represent the distorted shape of the initially straight SG, as shown in Figure 2.1b.

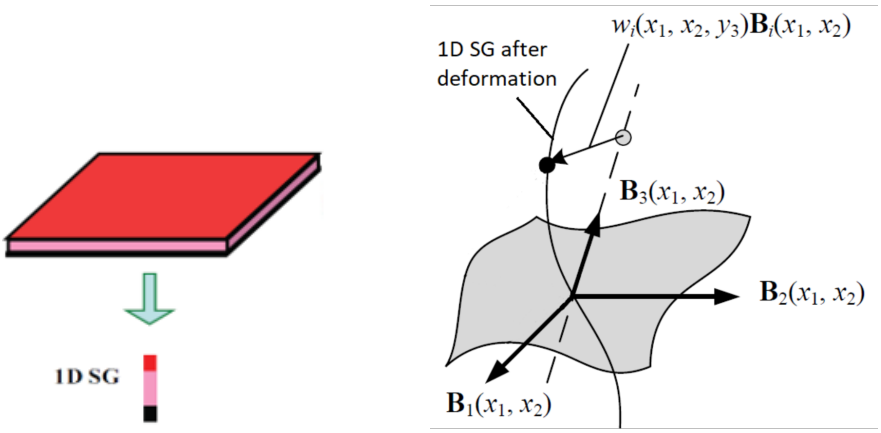

(a) 1D SG (b) Shell under deformation

Figure 2.1: 1D SG

For the MSG-based plate model, field measures are represented as functions of x_1 and x_2 defined over the reference surface, while x_3 is eliminated. We also use micro-coordinates y_i to describe the SG with $y_i = x_i/\varepsilon$ with ε being a small parameter.

In multiscale structural modeling, a field function of the original heterogeneous structure can be generally written as a function of the macro-coordinates x_k which remains in the macroscopic structural model and the micro-coordinates y_j. The partial derivative of a function $f(x_k, y_j)$ can be expressed as

$$\frac{\partial f(x_k, y_j)}{\partial x_i} = \frac{\partial f(x_k, y_j)}{\partial x_i}|_{y_j=const} + \frac{1}{\varepsilon}\frac{\partial f(x_k, y_j)}{\partial y_j}|_{x_k=const} \equiv f_{,i} + \frac{1}{\varepsilon}f_{|i} \tag{2.1}$$

The 3D displacement field field can be expressed in terms of the 2D displacements variable as :

$$\begin{gathered} u_1(x_1, x_2, y_1, y_2, y_3) = \overline{u}_1(x_1, x_2) - \varepsilon y_3 \overline{u}_{3,1}(x_1, x_2) + \varepsilon w_1(x_1, x_2, y_1, y_2, y_3) \\ u_2(x_1, x_2, y_1, y_2, y_3) = \overline{u}_2(x_1, x_2) - \varepsilon y_3 \overline{u}_{3,2}(x_1, x_2) + \varepsilon w_2(x_1, x_2, y_1, y_2, y_3) \\ u_3(x_1, x_2, y_1, y_2, y_3) = \overline{u}_3(x_1, x_2) + \varepsilon w_3(x_1, x_2, y_1, y_2, y_3) \end{gathered} \tag{2.2}$$

where u_i and $\overline{u}_i$ denote the displacements of the original 3D heterogeneous structure and the 2D plate model respectively. w_1, w_2, and w_3 are the unknown fluctuating functions, which are used to describe the displacement field that cannot be captured by the traditional Kirchhoff-Love plate model [18].

The infinitesimal strain field in the 3D linear elasticity theory can be defined as:

$$\varepsilon_{ij} = \frac{1}{2}(\frac{\partial u_i}{\partial x_j} + \frac{\partial u_j}{\partial x_i}) \tag{2.3}$$

Plug Eq. (2.2) into Eq. (2.3), the 3D strain field can be expressed using plate strain strains, curvatures, and fluctuating functions as:

$$\begin{gathered} \varepsilon_{11} = \epsilon_{11} + \varepsilon y_3 \kappa_{11} + w_{1|1} + \varepsilon w_{1,1} \\ \varepsilon_{22} = \epsilon_{22} + \varepsilon y_3 \kappa_{22} + w_{2|2} + \varepsilon w_{2,2} \\ \varepsilon_{33} = w_{3|3} \\ 2\varepsilon_{12} = 2\epsilon_{12} + 2\varepsilon y_3 \kappa_{12} + w_{1|2} + w_{2|1} + \varepsilon w_{1,2} + \varepsilon w_{2,1} \\ 2\varepsilon_{13} = w_{1|3} + w_{3|1} + \varepsilon w_{3,1} \end{gathered} \tag{2.4}$$

$$2\varepsilon_{23} = w_{2|3} + w_{3|2} + \varepsilon w_{3,2}$$

where the plate strains $\epsilon_{\alpha\beta}$ and curvatures $\kappa_{\alpha\beta}$ are defined as:

$$\epsilon_{\alpha\beta}(x_1, x_2) = \frac{1}{2}(\overline{u}_{\alpha,\beta} + \overline{u}_{\alpha,\beta}); \kappa_{\beta\alpha}(x_1, x_2) = -\overline{u}_{3,\alpha\beta} \tag{2.5}$$

Th,e potential energy of the 3D structure can be defined as:

$$\Pi = \frac{1}{2}\int_S U_{2D} ds - W \tag{2.6}$$

where W is the work done by external sources. U_{2D} is the 2D strain energy density defined as:

$$U_{2D} = \frac{1}{2\omega} < \sigma_{ij}\varepsilon_{ij} > \tag{2.7}$$

where ω denotes the area spanning the $y_1 - y_2$ plane of the SG. The fluctuating functions follow the constraints:

$$< w_i >= 0 \tag{2.8}$$

By minimizing the potential energy, the fluctuating functions w_i are solved [22]. The 2D kinetic variables called the plate stress resultants are defined as:

$$\begin{aligned} \frac{\partial U_{2D}}{\partial \epsilon_{11}} = N_{11}; \frac{\partial U_{2D}}{\partial 2\epsilon_{12}} = N_{12}; \frac{\partial U_{2D}}{\partial \epsilon_{22}} = N_{22} \\ \frac{\partial U_{2D}}{\partial \kappa_{11}} = M_{11}; \frac{\partial U_{2D}}{\partial 2\kappa_{12}} = M_{12}; \frac{\partial U_{2D}}{\partial \kappa_{22}} = M_{22} \end{aligned} \tag{2.9}$$

The plate constitutive equation that relates the plate stress resultants and strain measures can be obtained as:

$$\begin{Bmatrix} N_{11} \\ N_{22} \\ N_{12} \\ M_{11} \\ M_{22} \\ M_{12} \end{Bmatrix} = \begin{Bmatrix} A_{11} & A_{12} & A_{16} & B_{11} & B_{12} & B_{16} \\ A_{12} & A_{22} & A_{26} & B_{12} & B_{22} & B_{26} \\ A_{16} & A_{26} & A_{66} & B_{16} & B_{26} & B_{66} \\ B_{11} & B_{12} & B_{16} & D_{11} & D_{12} & D_{16} \\ B_{12} & B_{22} & B_{26} & D_{12} & D_{22} & D_{26} \\ B_{16} & B_{26} & B_{66} & D_{16} & D_{26} & D_{66} \end{Bmatrix} \begin{Bmatrix} \epsilon_{11} \\ \epsilon_{22} \\ 2\epsilon_{12} \\ \kappa_{11} \\ \kappa_{22} \\ 2\kappa_{12} \end{Bmatrix} \tag{2.10}$$

Here, the 6×6 plate stiffness matrix is composed of the $\boldsymbol{A}$, $\boldsymbol{B}$ and $\boldsymbol{D}$ matrices. Although the same notation of $\boldsymbol{A}$, $\boldsymbol{B}$ and $\boldsymbol{D}$ matrices is used from Classical Lamination Theory (CLT), the way to obtain these stiffness matrices has no relation to that has been used to derive CLT. This stiffness matrix is used as input to conduct the macroscopic plate analysis.

2.2 Framework

First, a structural model is generated in Abaqus. The mesh is generated for the FE model. The design setups, like fiber paths, layup sequence, optimization method, objective function, and constraints are defined using the developed GUI plug-in. The fiber angle function for each layer is homogenized to an SG and then the information is compiled in form of an ABD matrix to find effective properties at every elemental level to calculate u_e, as shown in Figure 2.2.

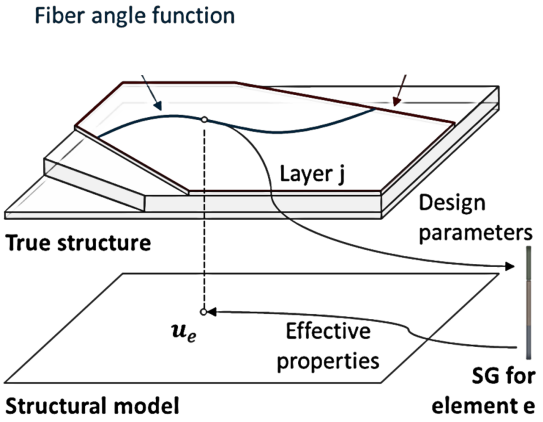

Figure 2.2: Fiber orientation, SG, and structural model

After the design setups, the GUI plug-in calls external codes. The design setups are used to generate a master design file which contains all the design setups and necessary parameters for multiscale modeling and optimization. The FE input files are generated from the structural model. For Abaqus, the required input file is an INP file. Then, the GUI plug-in calls SwiftComp which runs the MSG plate modeling. The FE input files are then updated with the location-dependent shell element properties. The GUI plug-in is capable to run structural analysis. If the parametric study or optimization study is required, the GUI plug-in then calls a python script to run Dakota, an open-source design optimization code developed by Sandia

National Laboratories [23]. For the optimization analysis behind the GUI plug-in, Dakota controls the data flow between MSG plate modeling, structural analysis, and optimization.

Specifically, the shell element stiffness is computed by the MSG plate model based on the location-dependent fiber angles in tow-steered composite layers. The computed shell element stiffness of each element is read by Dakota and then Dakota updates the INP files with the new shell element stiffness and calls Abaqus to perform structural analysis. The structural responses are also read by Dakota and form the predefined objective function to be minimized.

The objective function along with other setups (e.g., constraints) are sent to a built-in optimizer in Dakota to update the design variables. Any optimizer can be selected in Dakota depending on the problems, a user might want to solve. After that, the next iteration from MSG plate modeling, structural analysis, and optimization will be automatically performed with the updated design variables. The framework is as outlined in Figure 2.3.

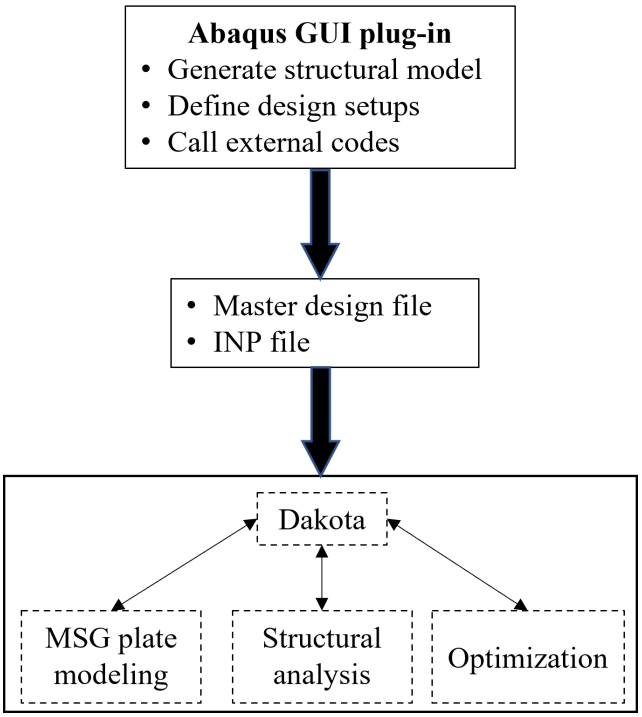

Figure 2.3: Design framework

Chapter 3

Development of GUI

The basic layout of the proposed GUI plug-in in Abaqus is shown in Figure 3.1. The “Advanced Tailorable Composites (ATC)" menu option in the Abaqus GUI plug-in contains the necessary modules. The "Microscale Modeling" module performs microscale homogenization analysis to compute effective properties of lamina based on fiber and matrix. The “Define fiber angles" module offers a flexible way to input any fiber angle expressions with arbitrary design variables. The “Structural analysis" module, as the name suggests, allows to run the structural analysis and perform a quick evaluation of the FE model with the design variables. The “Step" module is used to define the data transformation between the MSG plate modeling, FE structural analysis, and optimization. The “Parametric Study" module is used to describe the user-defined design space and the partition of the space to automatically iterate the structural analysis with different design variables. The “Optimization" module specifies the design variables, objective functions, constraints, and other parameters for complete optimization analysis.

3.1 Microscale modeling

The *Microscale Modeling* takes the fiber, matrix, and microstructure of composites for a homogenization analysis. There is a choice of a Square profile or a Hexagonal profile as a microstructure. The geometry of the microstructure or SG is defined either by describing the volume fraction or the radius of the fiber. There is an option for defining interphase around the fiber, by describing the volume fraction or the thickness around the fiber. The *model name* is chosen, to specify the model that would

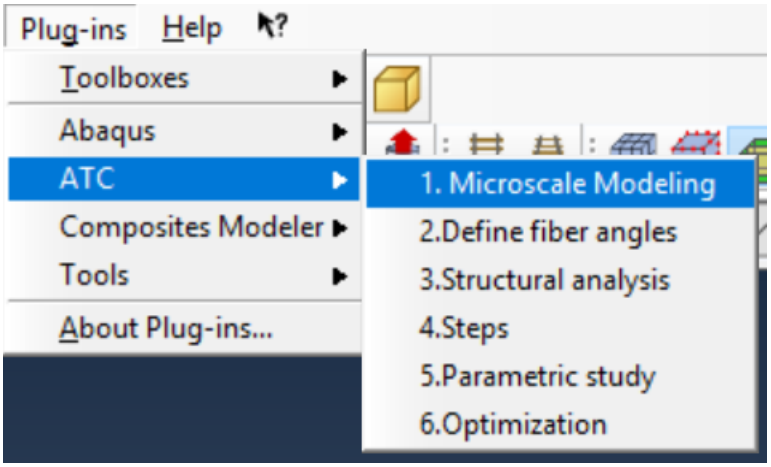

Figure 3.1: Abaqus GUI plug-in

need the effective lamina properties from the microscale homogenization. The material is assigned using the predefined material properties from the FE model tree for the fiber, the matrix, and the interphase (if needed). The mesh size and mesh element type are also specified here. There is a choice of two types of analysis - *Elastic analysis* or *Thermoelastic analysis*. The *Microscale Modeling* window for the Square profile is outlined in Figure 3.2a and the Hexagonal profile window is outlined in Figure 3.2b.

All this information is compiled to be written in a format (.sc) that is run on SwiftComp directly from the GUI. After the SwiftComp run, the SG is generated on the Abaqus Viewport. At the same moment, new lamina properties are written as a new material for the selected model in Abaqus. This new material can further be utilized by other modules (e.g., define fiber angles).

3.2 Define fiber angles

The data structure of the definition of tow-steered composites is outlined in Figure 3.3. There are two attributes associated with laminate objects: Regions and Layup. The regions are defined via element sets in Abaqus. Different laminates can be assigned to different element sets, and therefore FE structure can be made by laminates with different layups. The layup can be defined using conventional expressions in laminate, such as $[l_1/l_2/l_3/...]$ as shown in Figure 3.3. "l_1" is the name of the lamina object, the lamina object has attributes: orientation, thickness, and material. The

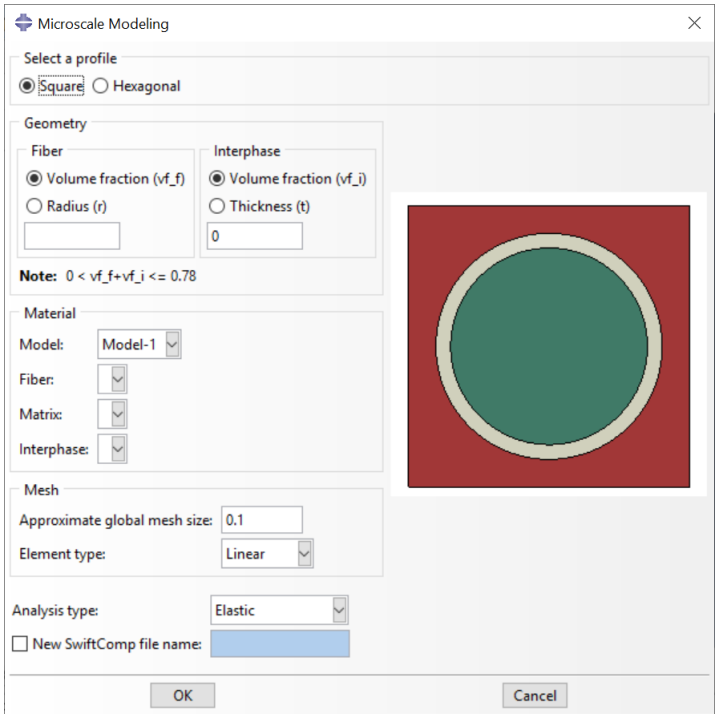

(a) Square pack SG

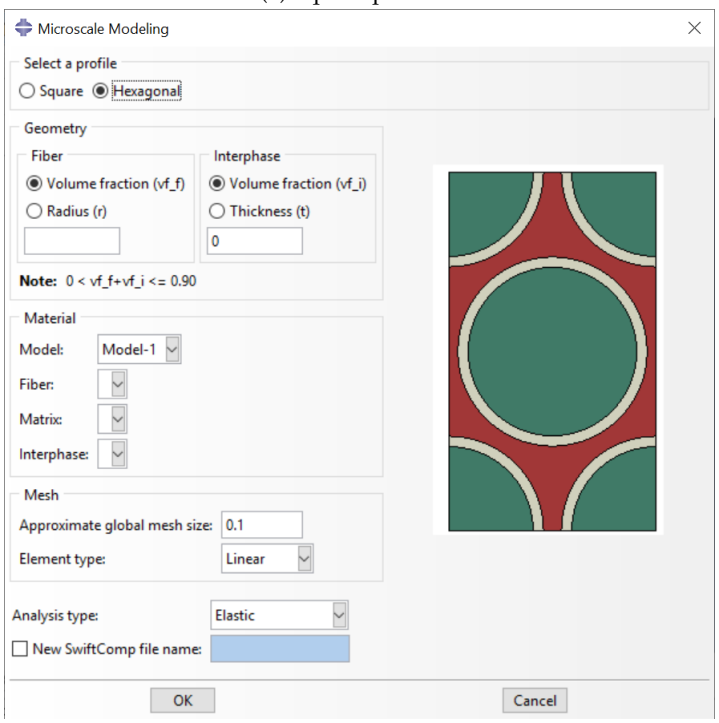

(b) Hexagonal pack SG

Figure 3.2: Microscale modeling window box

thickness of the lamina is specified, along with the applicable material property. The orientation object describes the fiber path in a lamina. The angle orientations can be a constant, a one-line expression, or be defined using external python scripts. The constant angle is for the traditional unidirectional fiber-reinforced composites. The

one-line expression is for a fiber path defined using a single function. The external scripts can be used to define a complex fiber path that cannot be expressed with a single function. An arbitrary fiber path with different complexities can be defined using this method.

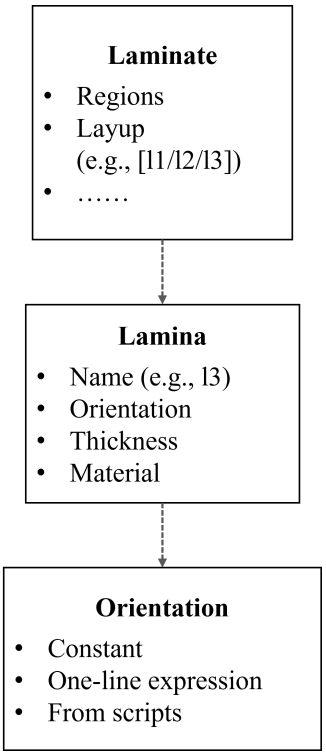

Figure 3.3: Data structure for fiber angles

In the *Define fiber angles* window (Figure 3.4), at first, layers with customized fiber angle orientations are defined in the form of a constant angle, a one-line expression, or advanced scripts. The predefined lamina properties in the FE model are chosen using the material name. The layer thickness is also defined in this window. The failure criterion can also be provided for failure analysis to predict the failure index and strength ratio which can be used as a constraint for the design optimization. After defining all the layers, the "Layup" functionality is used to define the sequence in the laminate. The layup can be defined using the index or name of a defined layer. Then, the defined laminate is assigned to a region or multiple regions in the FE model.

It is possible to replace conventional laminate region in an existing FE model with tow-steered composites. In this case, the complexities of tow-steered laminate

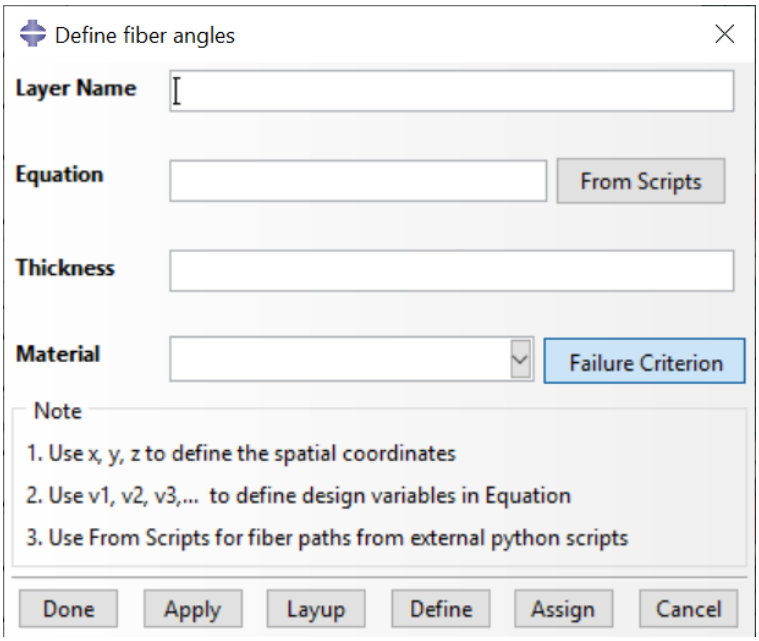

Figure 3.4: Define fiber angles window box

are defined via the *Define fiber angles* window of the GUI and assigned to those regions. Only some minor modifications of the original model are required such as defining an element set for the regions and defining a new material property for the lamina if needed. Secondly, FE models with multiple types of elements (e.g., solid, shell, and beam elements) can also be analyzed with the developed GUI, because only the properties of shell elements need to be re-defined while the rest of the FE model remains the same.

Additionally, the fiber angles that cannot be expressed by a constant or a one-line expression can be defined using the *From Scripts* button of *define fiber angles* window that pops up the window as shown in Figure 3.5. The "File_name" is the python file name that contains the functions needed to define the fiber angles. This "Function_name" is the name of the function that uses the design coefficients and design parameters to convert data to the corresponding fiber angle orientations. The "Transformation" is a function that can contain the details about the axis transformation for fiber angles if needed. A multiplier can also be described here to incorporate the negative of the input fiber angle variables directly because $\pm\theta$ layups are commonly used to define quasi-isotropic laminates. The layer name, thickness, and material are defined in the *define fiber angles* window to complete the input for a specific layer.

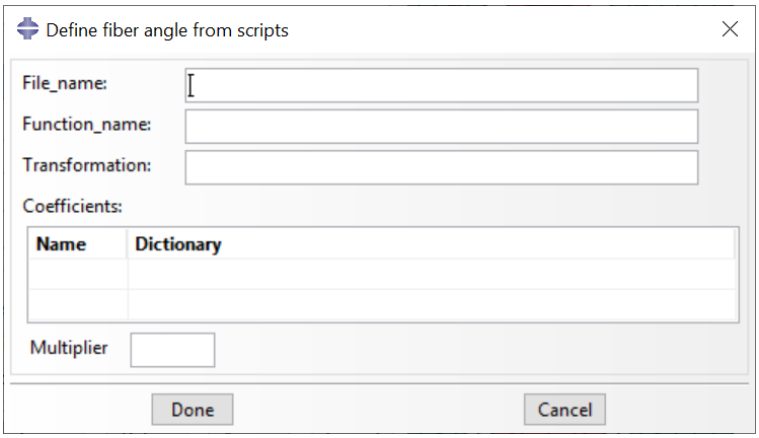

Figure 3.5: *From Scripts* window box

3.3 Structural analysis

A one-time structural analysis is provided by this module. Before running a more time-consuming analysis, this function is intended to quickly evaluate the design settings. Besides, a one-time structural analysis can also be used to estimate the whole computing expense for more computationally expensive jobs such as parameter study and optimization. After saving the model job file (*inp file*) and saving design setups, all the information is compiled to write a Master Design file as shown in Figure 2.3. The name of the job file is input in the structural analysis window, as shown in Figure 3.6 and the analysis can be carried out.

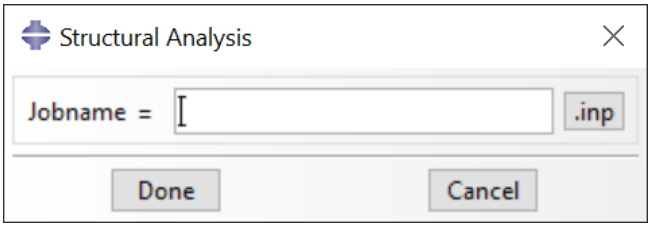

Figure 3.6: Structural analysis window box

3.4 Parametric study

This module can be used to look into how design parameters behave. The computational time can be controlled by the number of partitions of the design variables. The parameter study is performed to understand the distribution of the structural response of interest (e.g., displacements in a nodal set). For more advanced analysis such as parameter study of a buckling load, scripts and more parameters need to be

defined in the Steps module. The distribution of structural responses helps to tailor the optimization parameters (e.g., reduce the range of design variables) to reduce the computational costs. The parametric study window snippet is shown in Figure 3.7.

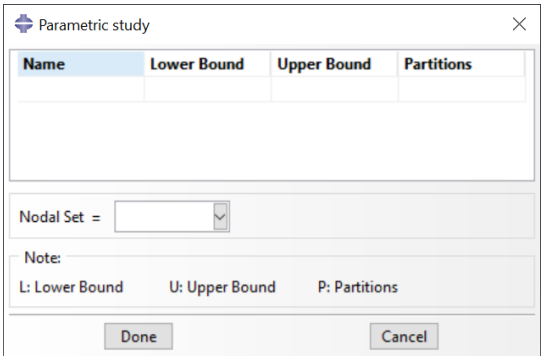

Figure 3.7: Parametric study window box

In this window, the name of the design variables, their upper and lower bounds, and the number of their partitions are specified. Any nodal set of interest that is pre-defined in the FE model, is selected here. When *Done* is clicked on this window, the parametric study is carried out and when finished, the design parameters' influence on the interest points is written in an external file that can be used to select optimization parameters.

3.5 Steps

When dealing with complex FE analysis, some steps need to be defined for Abaqus and python scripts. For Abaqus, the job file name of the saved model (*.inp file*) is selected. For post-processing purposes, a predefined python file is selected, that contains the information about the results post-processing. These scripts specify unique formats that the results related to tow-steering fiber paths can be stored, as shown in Figure 3.8a. For Python, another predefined python file is defined that can contain many functions. The function variables and their respective values can be input in the window, as shown in Figure 3.8b. These scripts are used to calculate specified properties for the fiber paths or orientations.

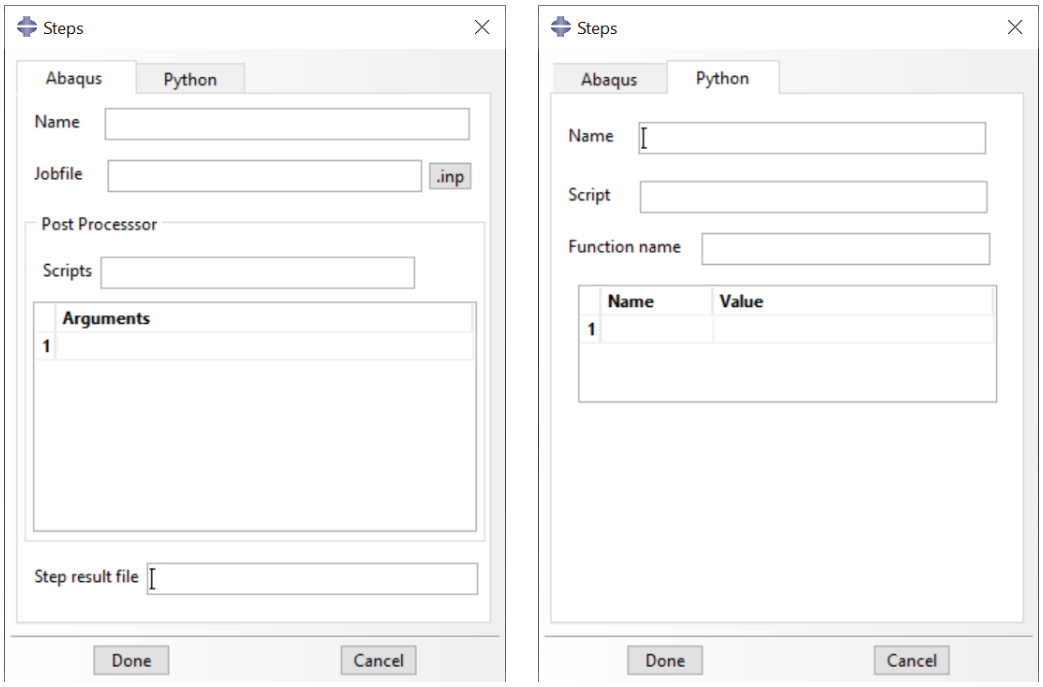

(a) Abaqus Steps (b) Python Steps

Figure 3.8: Steps window box

3.6 Optimization

For optimization, the method can be selected, either a Single-objective Genetic Algorithm (SOGA) or a Multi-objective Genetic Algorithm (MOGA) provided by Dakota [23]. The population size, the number of maximum evaluations, the number of seeds, and the print style for each population of design variables are set, as in Figure 3.9a. All the design variables for defined fiber angles are given lower and upper bounds that specify the parameter set to be iterated by a particular method, as in Figure 3.9b. Some specific responses that need to be monitored are defined in the third tab. These responses include a description of the model output information that Dakota received after an interface evaluation. Any constraint with its value or behavior, as well as a descriptor and its sense, can be entered, as in Figure 3.9c.

The parameters specified in this module are also written into the Master Design file, which the plug-in uses to call Dakota to perform optimization. For simple optimization problems, the objective function and constraints can be defined in the Optimization GUI window, but to define necessary parameters for complex optimization problems, additional parameters, and python scripts are used to be defined in the Steps module.

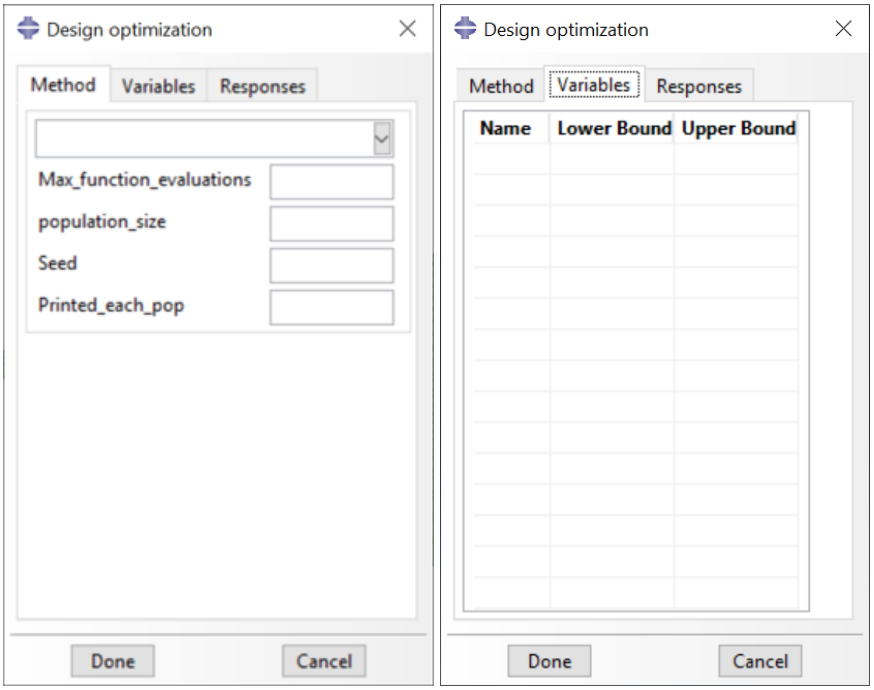

(a) Optimization methods (b) Variables

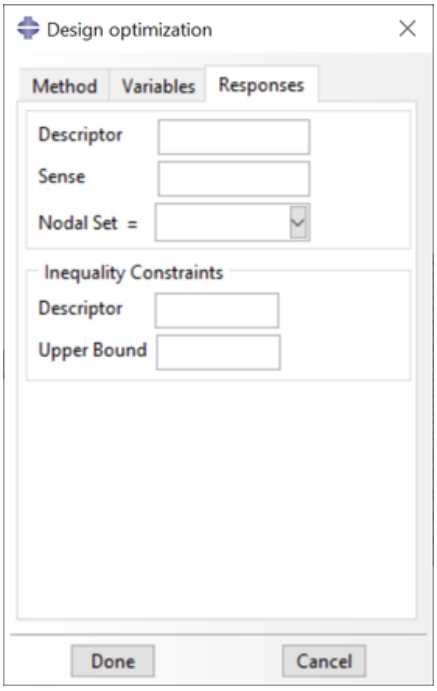

(c) Responses

Figure 3.9: Optimization window box

Chapter 4

Examples

4.1 Example I - Structural Analysis

4.1.1 Problem statement

In this problem, a cantilever plate is analyzed to demonstrate the structural analysis module of the developed GUI. Here, the cantilever plate is divided into two regions. One region has a two-layer conventional laminate with a [0/90] layup, and the other region has a two-layer tow-steered composite laminate. The two regions are shown in Figure 4.1. With the developed GUI, it is not required that the overall structure be made by variable stiffness laminates entirely. For realistic structures, there are usually many regions with different laminates and materials. Users can solve only some regions to be replaced by variable stiffness laminates and this GUI can handle that case. In this particular case, as there are two regions, the goal is to demonstrate that the efforts are minimized when trying to solve this kind of problem.

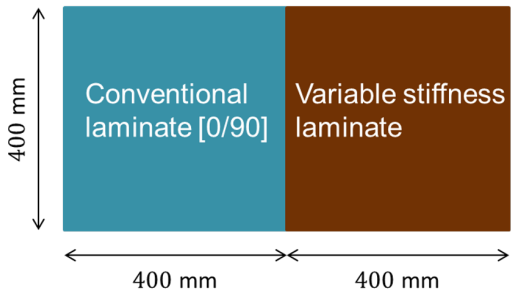

Figure 4.1: Dimensions of the cantilever plate

A uniform pressure of $1e^{-10}N/mm^2$ is applied on the top surface of the plate, and one end is clamped as shown in Figure 4.2.

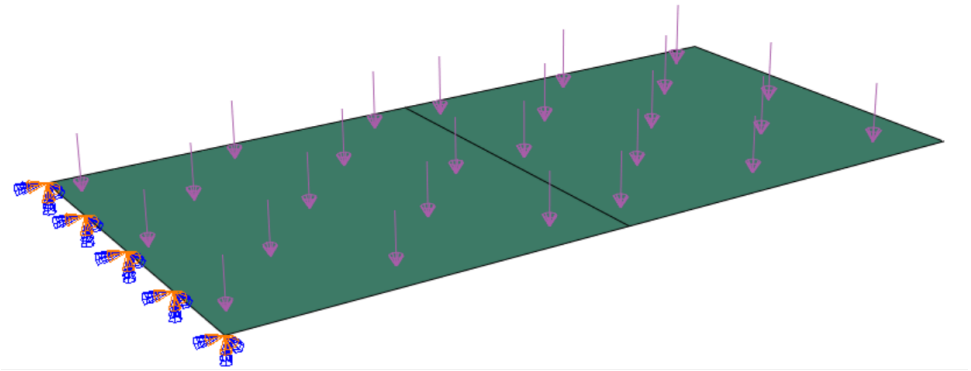

Figure 4.2: Boundary conditions

4.1.2 Using the GUI plug-in

Microscale modeling

Using the Microscale modeling module of the developed GUI, the lamina properties can be computed based on fiber and matrix. In this example, a composite of carbon fiber is used with epoxy resin. The properties of fiber and matrix are as in Table 4.1. The volume fraction of fiber is 0.64, to replicate the paper [18]. A linear mesh element of 0.05 mesh element size is selected, as shown in Figure 4.3.

Table 4.1: Properties of fiber and matrix

Properties	T300 carbon fiber	Epoxy resin (matrix)
E_1 (MPa)	230000	3450
$E_2 = E_3$ (MPa)	40000	3450
$G_{12} = G_{13}$ (MPa)	24000	1280
G_{23} (MPa)	14300	1280
$\nu_{12} = \nu_{13}$	0.26	0.35
ν_{23}	0.40	0.35

The SG can be generated on Abaqus Viewport, as shown in Figure 4.4a for a square pack SG with no interphase and Figure 4.4b for a hexagonal pack SG with no interphase. New lamina properties are written as new material in Abaqus that are utilized later.

The lamina properties for square profile SG and hexagonal profile SG obtained from "Microscale Modeling" are as shown in Table 4.2.

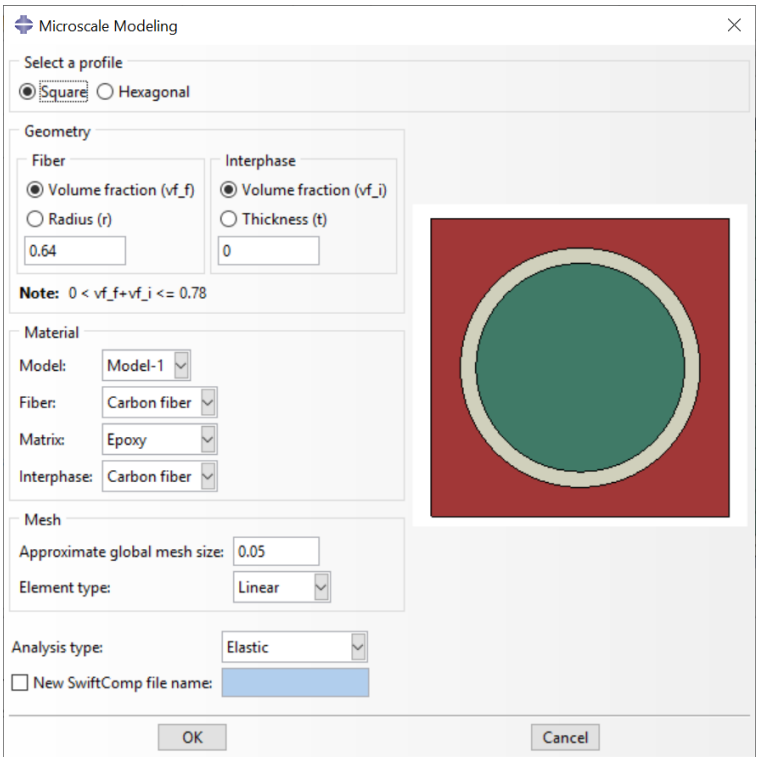

Figure 4.3: MSG modeling selections for square pack

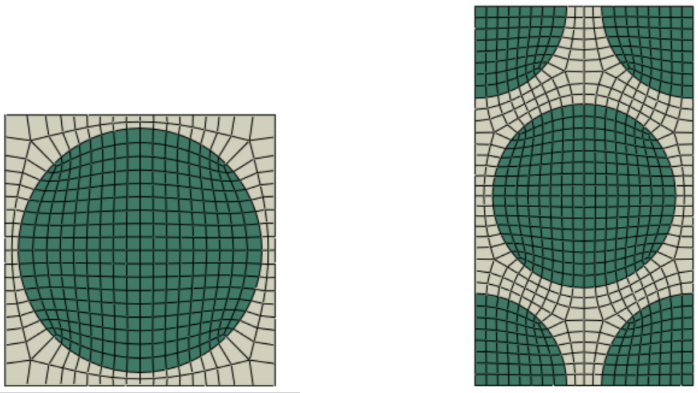

(a) Square Pack Structure Genome with no interphase

(b) Hexagonal Pack Structure Genome with no interphase

Figure 4.4: Microstructure

Structural analysis

The squared pack SG is used as lamina properties for structural analysis. The layer thickness of laminates is 0.127 mm each. The layup for tow-steered composite laminate has two layers. One-line expression is used for both layers. For the first layer, the fiber orientation is defined using the expression $[2 \times (v_2 - v_1) \times abs(x)/B + v_2]$, where v_2 and v_1 are design variables, B is the width of the plate and is equal to 400 mm. Layer 1 is defined via the GUI window as shown in Figure 4.5a. For the second

Table 4.2: Lamina properties for square and hexagonal profiles

Model	Square	Hexagonal
E_1 (MPa)	148214.16	148140.84
E_2 (MPa)	14431.80	11971.71
E_3 (MPa)	14430.99	11985.86
G_{12} (MPa)	5118.13	4761.53
G_{13} (MPa)	5118.04	4770.72
G_{23} (MPa)	3405.48	4169.49
ν_{12}	0.287	0.288
ν_{13}	0.286	0.288
ν_{23}	0.338	0.432

layer, the expression is defined as $[2 \times (v_2 - v_1) \times abs(y)/B + v_1]$, as in Figure 4.5b.

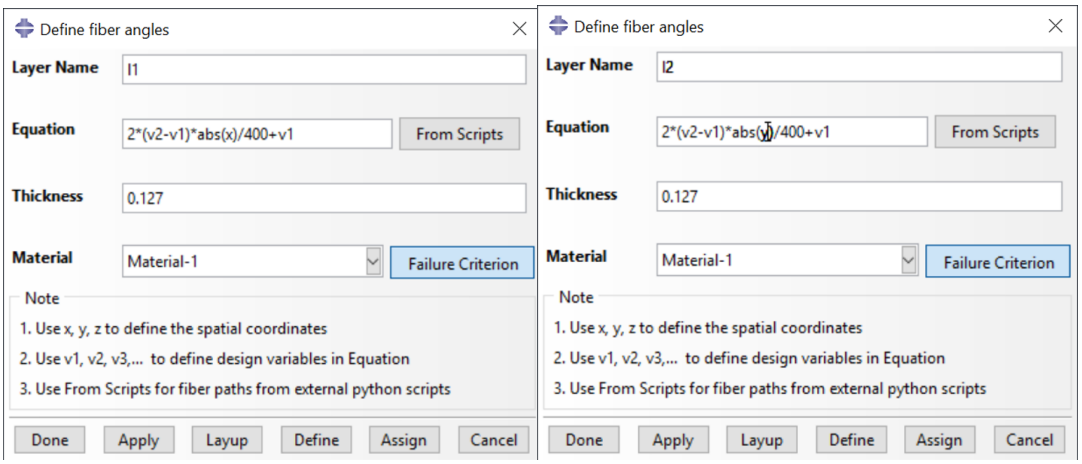

(a) Layer 1 (b) Layer 2

Figure 4.5: Layer definitions

The initial values for design variables v_1 and v_2 are 0 and 60. The fiber paths for the two layers are shown in Figure 4.6. The layup is defined in GUI as in Figure 4.7a. The conventional laminate region is called 'Set-1' and the other region with tow-steered composite laminate is called 'ATC'. After the declaration of initial values for the defined variables, the region for ATC is selected for the tow-steered composite laminate, as shown in Figure 4.7c.

Users need to save the FE structural model as an Abaqus INP file (*plate400.inp* in this case). From the structural analysis window, Figure 4.8, the job name is selected from the working directory. The structural analysis is then run in the command window. The structural analysis uses the element IDs, node and element connectivity, and material properties from the INP file, to solve for tow-steered composites. The structural analysis stops automatically when completed.

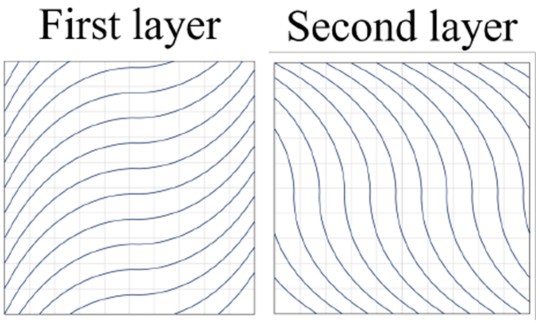

Figure 4.6: Fiber path of the first layer and the second layer

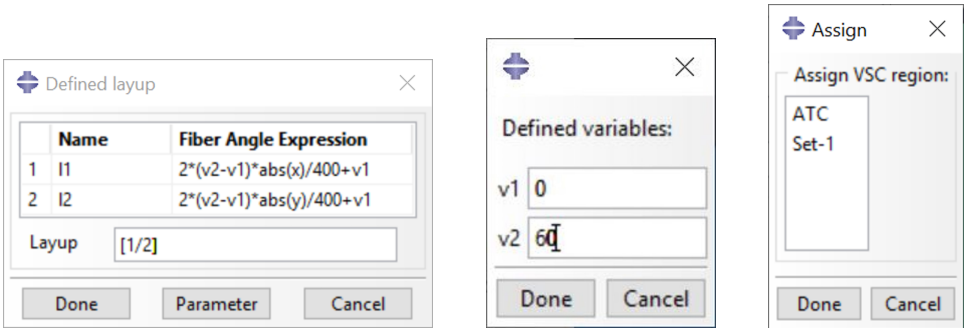

(a) Layup (b) Initial Values (c) Assign regions

Figure 4.7: Sub-windows of define fiber angles

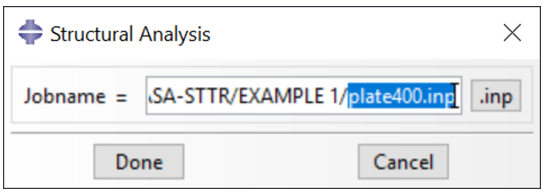

Figure 4.8: Structural analysis

4.1.3 Results

The *odb* file contains all the FE results. The displacement along the normal of the plate, u_3 is as shown in Figure 4.9. The plate is bent maximum at the free end.

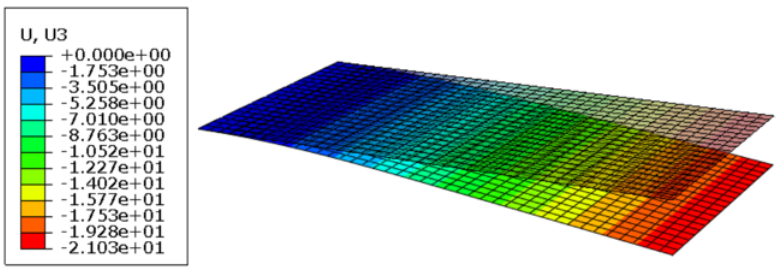

Figure 4.9: Displacement in z-axis direction

The section moment in the x-axis (SM_1), along the length of the plate, is as shown in Figure 4.10. The section moment is symmetrical for the uni-directional laminate

region about the center, whereas there is variation in distribution for the tailorable laminate region.

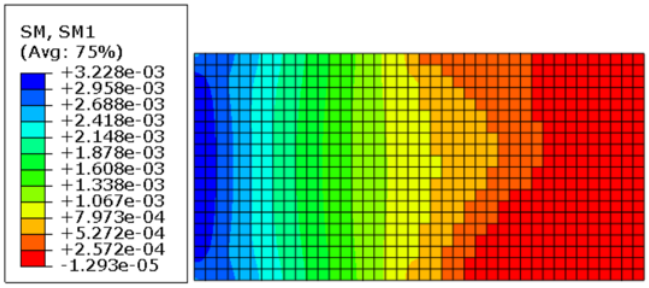

Figure 4.10: Section moment in the x-axis on the plate

4.2 Example II - Optimization

4.2.1 Problem statement

The buckling optimization of a pressurized cylindrical structure is carried out in this section. This structure is taken from the work of Blom et al. [24]. With in-plane curvature as a constraint, the aim is to maximize the buckling moment on this cylinder. The diameter of the cylinder is 24 inches and the length is 32 inches. There are 24 layers on the cylinder shell and 15 design variables. The layer thickness of the cylinder is 0.0072 inches each. The cylindrical FE model is as shown in Figure 4.11. There are two center nodes defined at each end and boundary conditions on each end have rigid elements linking all circumferential nodes to the simply-supported center node, as shown in Figure 4.11a and Figure 4.11b. A concentrated moment (1000 lb-in) is applied to each center node and the lower half is in compression, as shown in Figure 4.11c.

$$\cos\varphi(\theta) = \cos\varphi_i + (\cos\varphi_{i+1} - \cos\varphi_i)\frac{\theta - \theta_i}{\theta_{i+1} - \theta_i} \tag{4.1}$$

The circumferential coordinate θ that defines the fiber angle φ function, with respect to the longitudinal axis as in Eq. (4.1), is shown in Figure 4.12. The layup of the structure is $[\pm 45/\pm\varphi_1(\theta)/0/90/\pm\varphi_3(\theta)/0/90/\pm\varphi_5(\theta)]_S$. Each of the three layers defined by φ_i (i=1, 3, 5) have five design variables each - φ_{i0}, φ_{i1}, φ_{i2}, φ_{i3}, and φ_{i4}. The material properties are defined as elastic type with engineering constants -

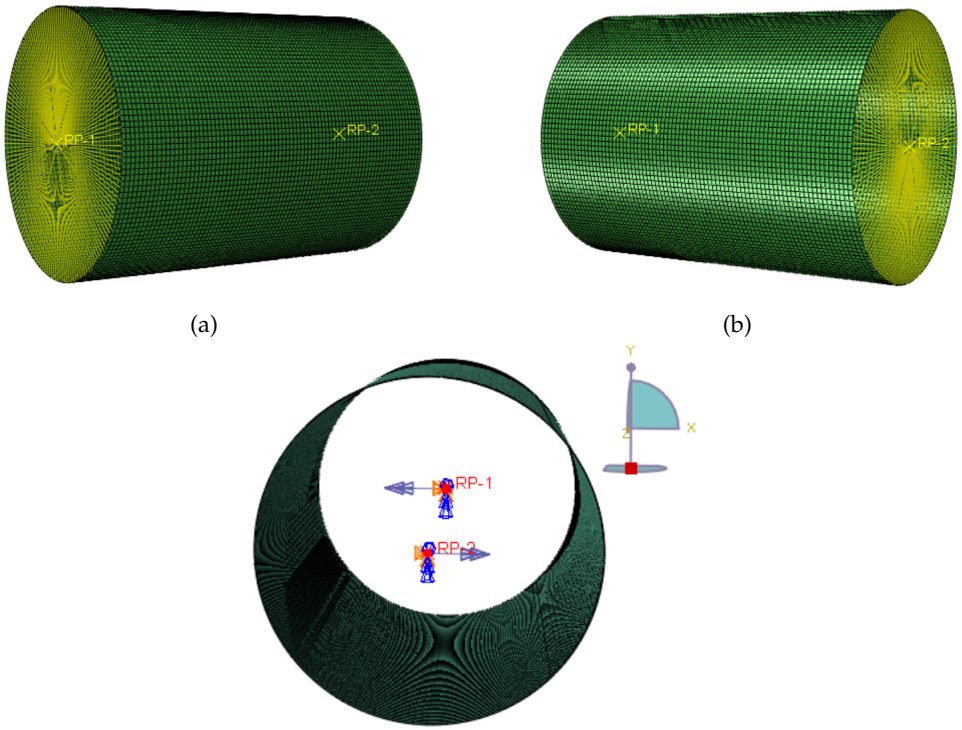

(a) (b)

(c)

Figure 4.11: Cylindrical shell FE model

$E_1 = 18.83e^6$ psi, $E_2 = E_3 = 1.317e^6$ psi, $G_{12} = G_{13} = 7.672e^5$ psi, $G_{23} = 5.065e^5$ psi, $\nu_{12} = \nu_{13} = 0.32$, $\nu_{23} = 0.3$. The failure criterion based on *Tsai-Wu* criterion is declared here.

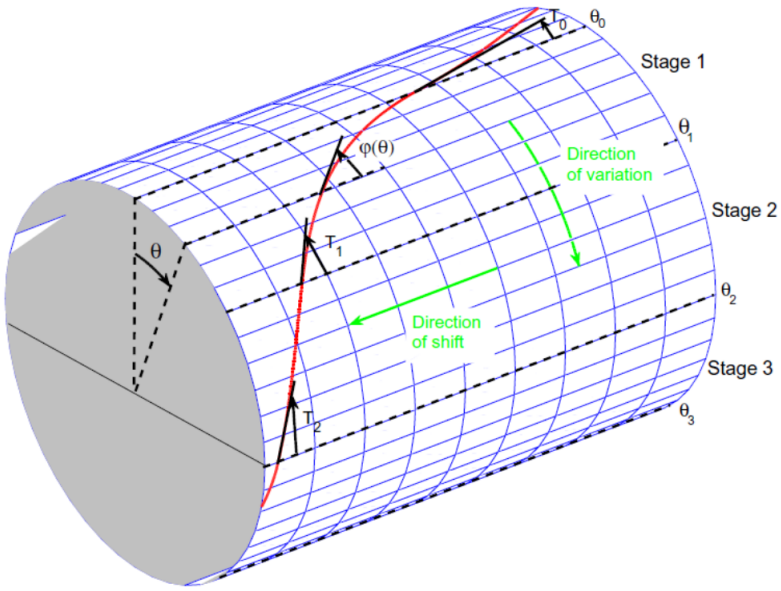

Figure 4.12: Cylindrical fiber path orientation

4.2.2 Using the GUI plug-in

The layup in this problem has the layers defined using a constant fiber angle or the scripts. The first two layer definitions, using constant fiber angles of 45° and -45°, are input in the *define fiber angles* window as shown in Figure 4.13a and Figure 4.13b. Similarly for layer *l5*, *l6*, *l9* and *l10*, the layer orientation is defined using constant angles.

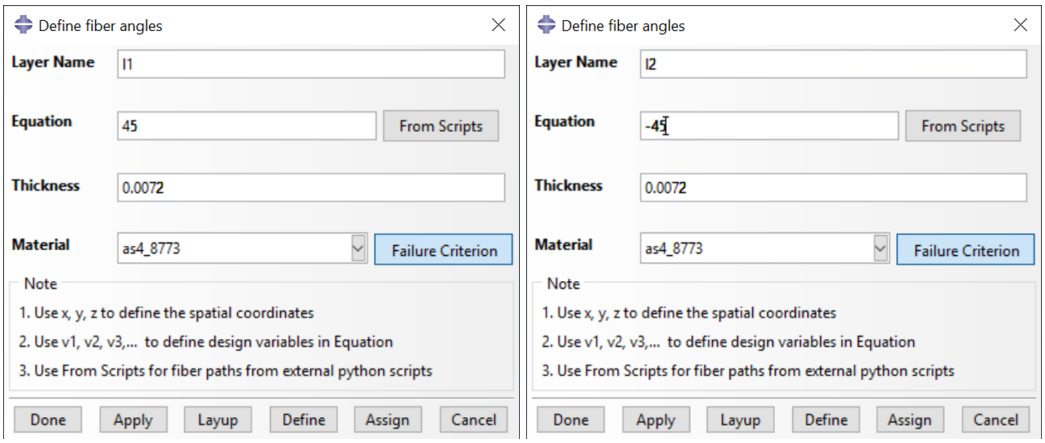

(a) Layer 1 (b) Layer 2

Figure 4.13: Layer definition

The fiber layers that need to be described using scripts (i.e, for layers *l3*, *l4*, *l7*, *l8*, *l11* and *l12*) are defined using windows as shown in Figure 4.14a. There are five design variables for each of $\phi_i (i = 1, 3, 5)$. The file name *users_function* is the python file name that contains the function *svFiberAngle*. This function converts the provided coefficients θ and design variable ϕ angle values to the corresponding fiber angle orientations. The failure criterion is declared using Figure 4.15 as in the work

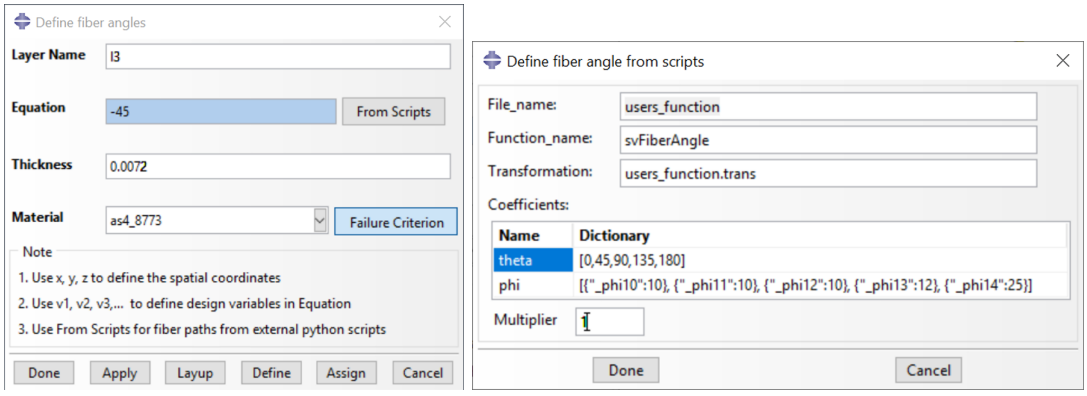

(a) Layer 3 (b) From Scripts

Figure 4.14: Layer 3 with script definitions

of Blom et al. [24]. The failure criterion based on *Tsai-Wu* criterion is chosen here. The strength value coefficients for $X_t = 29900$ MPa, $Y_t = Z_t = 19250$ MPa, $X_c = 168000$ MPa, $Y_c = Z_c = 28980$ MPa, $R = T = 16880$ MPa, $S = 12060$ MPa.

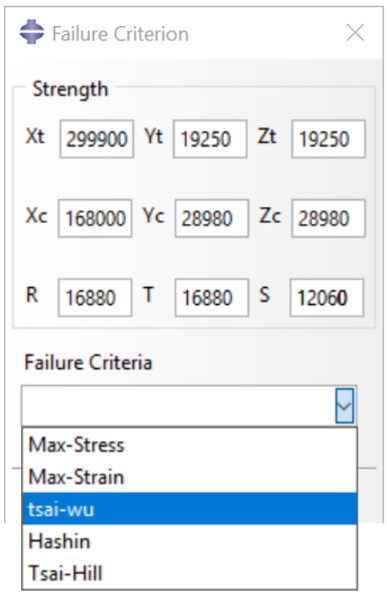

Figure 4.15: Failure criterion

The layup defined in the *layup* window for this example is input as shown in Figure 4.16.

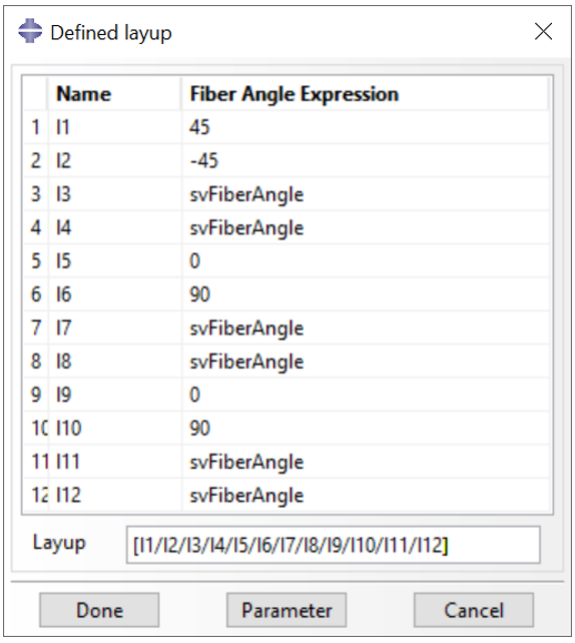

Figure 4.16: Layup for cylindrical buckling

For this example, the required steps need to be defined for Abaqus and python scripts. For Abaqus, the job file name of the saved model (*.inp file*) is selected. For

post-processing, *abq_get_result.py* is defined, which contains the information about results post-processing, as shown in Figure 4.17a. For Python, *users_function.py* is defined that can contain many functions. The function used here is *calcMaxCurvature*, which calculates the largest curvature allowed for θ equal to [0, 45, 90, 135, 180] for each design variable $\varphi_{i0}, \varphi_{i1}, \varphi_{i2}, \varphi_{i3}, \varphi_{i4}$ of the three layers (i=1, 3, 5) defined using scripts.

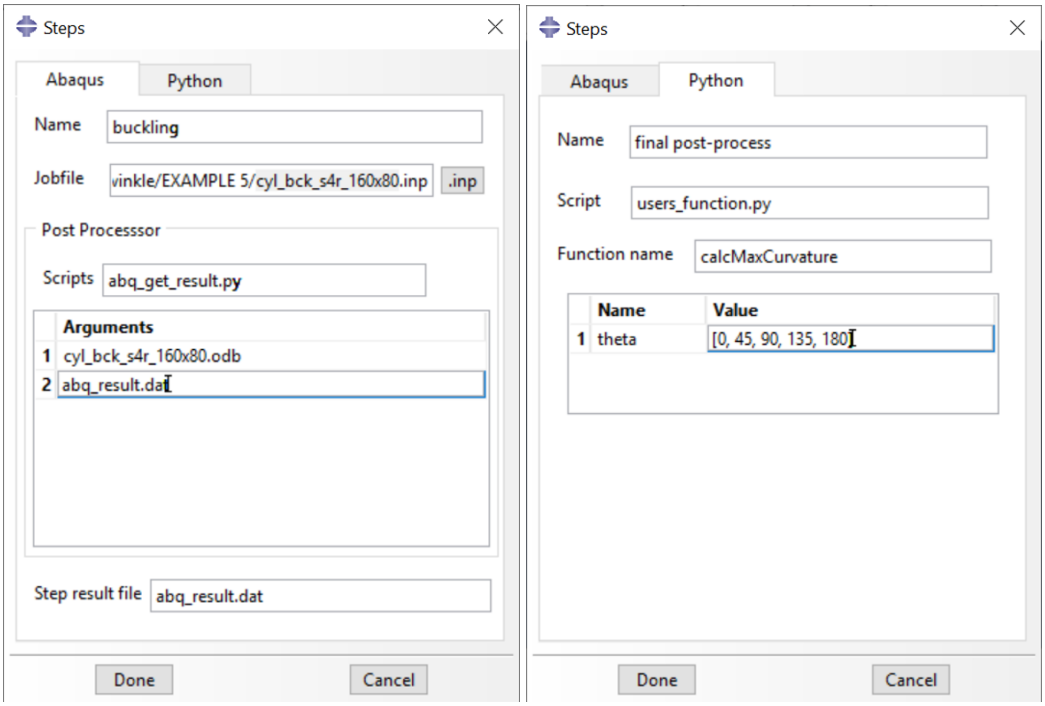

(a) Abaqus Steps (b) Python Steps

Figure 4.17: Steps window

The Single Objective Generic Algorithm (SOGA) method of Dakota is used for bucking optimization. For this example, the number of maximum evaluations to be run is equal to 10 and the population size is 5. The number of seeds is 1027 and each population is set to be printed after each population calculation. The optimization method selection is shown in Figure 4.18a. All the design variables for fiber angles are given lower bounds and upper bounds, as in Figure 4.18b. Here, the lower bound and upper bounds are 10 and 89 for all the variables. Some specific responses that need to be monitored are defined here, in Figure 4.19a. A descriptor named *mcr* is constrained to be *max*. Another descriptor for inequality constraint is named *curv_max* and is bounded to a value of 0.05 maximum.

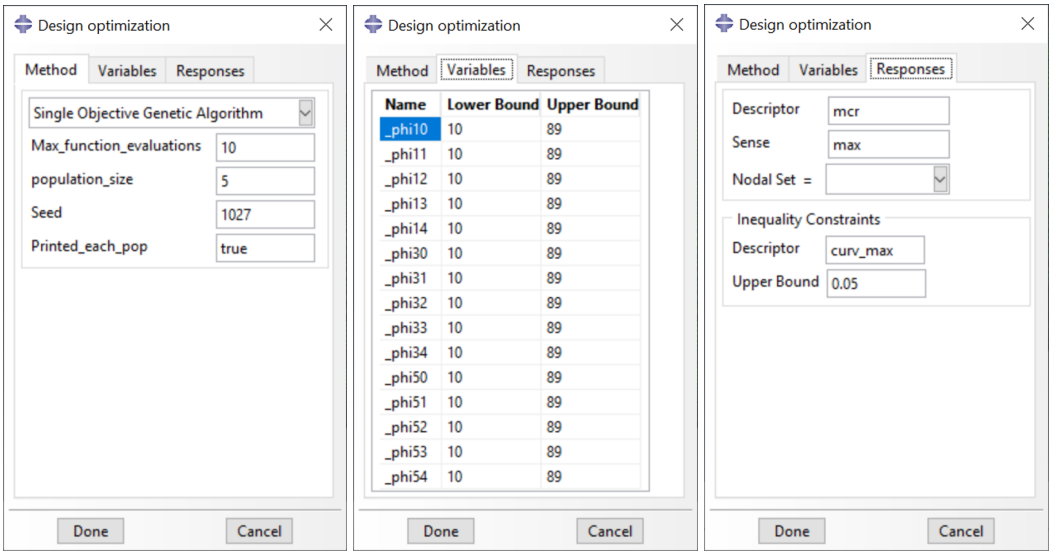

(a) Methods (b) Variables (c) Responses

Figure 4.18: Design optimization window

4.2.3 Results

The optimized results for each evaluation for all design variables and constraints are written in output files. Their updated values after each evaluation for the design variables with the constraints are as shown in Figure 4.19. This example has a limited number of evaluations to only depict the utilization of the developed GUI. The number of evaluations can be increased, and the final result can be applied to the model for analysis and final fiber tow placement on the cylinder laminate structure.

The deformation in cylinder structure in the 10^{th} evaluation is as shown in Figure 4.20.

%eval_id	interface	_phi10	_phi11	_phi12	_phi13	_phi14
1	NO_ID	18.17798395	18.47694327	52.58241523	30.22315134	53.0573748
2	NO_ID	20.18390454	47.6351207	61.02319407	60.86648152	26.13174841
3	NO_ID	54.34482864	49.53254799	35.58272042	27.23596912	16.43244728
4	NO_ID	62.65541551	24.93108921	53.9132664	25.69054231	81.18848231
5	NO_ID	80.19757683	72.45356609	31.90600299	47.0540788	69.06857509
6	NO_ID	20.18390454	49.53254799	61.02319407	60.86648152	16.43244728
7	NO_ID	25.56758324	47.6351207	61.02319407	60.86648152	26.13174841
8	NO_ID	54.34482864	47.6351207	35.58272042	60.86648152	26.13174841
9	NO_ID	54.34482864	49.53254799	31.90600299	27.23596912	69.06857509
10	NO_ID	80.19757683	72.45356609	35.58272042	27.23596912	69.06857509

(a)

_phi30	_phi31	_phi32	_phi33	_phi34	_phi50
43.95599231	73.54332102	28.9549852	74.60655538	29.29251991	52.89825129
20.98193304	21.92220832	23.85338908	80.5953856	84.86761071	81.7960448
44.16333506	35.1559801	14.70378735	48.70317698	24.57908872	73.46134831
74.67888424	68.33805353	27.31070894	72.04370251	39.83806879	32.09646901
43.16519669	23.41941588	29.66139714	60.4783166	29.2105472	60.54100162
20.98193304	21.92220832	23.85338908	80.5953856	84.86761071	81.7960448
20.98193304	21.92220832	23.85338908	80.5953856	84.86761071	81.7960448
44.16333506	35.1559801	23.85338908	48.70317698	24.57908872	73.46134831
43.16519669	35.1559801	14.70378735	60.4783166	24.57908872	60.54100162
43.16519669	35.1559801	14.70378735	60.4783166	24.57908872	60.54100162

(b)

_phi51	_phi52	_phi53	_phi54	mcr	curv_max
28.80550554	81.22946867	57.09573656	22.92275765	4049.1	0.0383978722
81.63692129	11.12833033	61.39448225	55.49244667	4618.2	0.04433801202
38.44694357	40.62886441	81.08239998	10.93545335	3790.8	0.04386456961
40.01165807	59.84423353	74.17017121	25.55552843	4130.6	0.03968072813
67.22659993	44.91073336	48.85024567	79.88897366	4562.6	0.02904247205
81.63692129	40.62886441	81.08239998	55.49244667	4642.6	0.03985122129
81.63692129	11.12833033	61.39448225	55.49244667	4679.8	0.04433801202
38.44694357	40.62886441	81.08239998	10.93545335	3502.8	0.04386456961
67.22659993	44.91073336	81.08239998	79.88897366	4697.2	0.02934783907
38.44694357	40.62886441	48.85024567	79.88897366	4696.4	0.02821705278

(c)

Figure 4.19: Design variable results for all evaluations

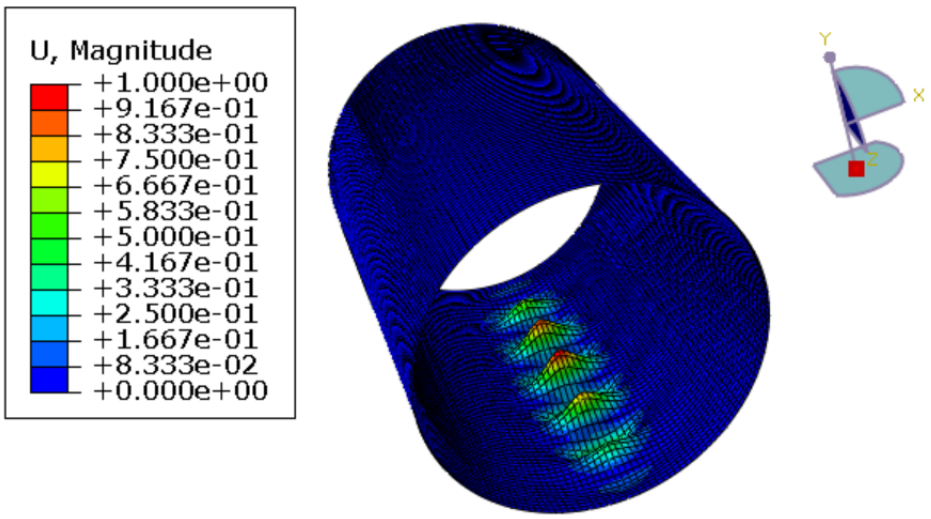

Figure 4.20: Displacement in cylinder structure

Chapter 5

Conclusion

5.1 Summary

The use of tow-steered composites could improve the mechanical performance of aerospace structures. The developed GUI plug-in meets the urgent need for an effective, user-friendly design tool for tow-steered composite structures. The plug-in provides for the definition of all design setups, greatly reducing the additional programming effort involved in alternate methods. The lamina properties can be calculated for square and hexagonal profiles, and the obtained material properties can be applied to the FE model. There are three ways to insert equations- constant angle, one-line expression, and using scripts; for arbitrary fiber angles of different complexities in the "Define fiber angles" module. Additionally, there is flexibility to choose which region(s) in a FE model needs to be assigned with the defined laminate. The plug-in provides with different analysis modules such as structural analysis, parametric study, and optimization study. Each analysis module serves a different purpose for the design and analysis of tow-steered composite structures, with a varied processing cost.

To illustrate the accessibility and adaptability of the developed design tools, two examples were provided, to demonstrate their application and power. The developed GUI plug-in can help analyze complex problems, just by using this unified environment for commercial FE.

5.2 Future work

- Currently the developed GUI works for elastic problems, it can be extended to thermoelastic problems or other very complex problems.
- Machine Learning can be employed to solve the computational issue for very large models and facilitate the process.
- The GUI plug-in can be made more compact, with increased robustness and a better interface.
- More realistic examples can be tested to further mature the codes.

References

[1] *Variable Stiffness Composites | Aerospace Engineering Blog*.

[2] "Space Applications of Composite Materials 66". In: *Journal of Space Technology Vol. 8* (2018).

[3] Thiago A.M. Guimarães et al. "Supersonic flutter and buckling optimization of tow-steered composite plates". In: *ICME for Structures* 57 (1 Dec. 2018), pp. 397–407. ISSN: 00011452. DOI: 10.2514/1.J057282. URL: https://arc.aiaa.org/doi/10.2514/1.J057282.

[4] Dawn C. Jegley, Brian F. Tatting, and Zafer Gürdal. "Tow-steered panels with holes subjected to compression or shear loading". In: *Collection of Technical Papers - AIAA/ASME/ASCE/AHS/ASC Structures, Structural Dynamics and Materials Conference* 5 (2005), pp. 3453–3466. ISSN: 02734508. DOI: 10.2514/6.2005-2081. URL: https://arc.aiaa.org/doi/10.2514/6.2005-2081.

[5] K. Chauncey Wu et al. "Design and manufacturing of tow-steered composite shells using fiber placement". In: *Collection of Technical Papers - AIAA/ ASME/ ASCE/ AHS/ ASC Structures, Structural Dynamics and Materials Conference* (2009). ISSN: 02734508. DOI: 10.2514/6.2009-2700. URL: https://arc.aiaa.org/doi/10.2514/6.2009-2700.

[6] Olivia Stodieck et al. "Improved aeroelastic tailoring using tow-steered composites". In: *Composite Structures* 106 (Dec. 2013), pp. 703–715. ISSN: 0263-8223. DOI: 10.1016/J.COMPSTRUCT.2013.07.023.

[7] Bret K. Stanford, Christine V. Jutte, and K. Chauncey Wu. "Aeroelastic benefits of tow steering for composite plates". In: *Composite Structures* 118 (1 Dec. 2014), pp. 416–422. ISSN: 0263-8223. DOI: 10.1016/J.COMPSTRUCT.2014.08.007.

[8] Timothy R. Brooks, Joaquim R.R.A. Martins, and Graeme J. Kennedy. "High-fidelity aerostructural optimization of tow-steered composite wings". In: *Journal of Fluids and Structures* 88 (July 2019), pp. 122–147. ISSN: 0889-9746. DOI: 10.1016/J.JFLUIDSTRUCTS.2019.04.005.

[9] Stephen M Barr and Justin W Jaworski. "Optimization of tow-steered composite wind turbine blades for static aeroelastic performance". In: (2019). DOI: 10.1016/j.renene.2019.02.125. URL: https://doi.org/10.1016/j.renene.2019.02.125.

[10] Karanpreet Singh and Rakesh K. Kapania. "Optimal design of tow-steered composite laminates with curvilinear stiffeners". In: *AIAA/ASCE/AHS/ASC Structures, Structural Dynamics, and Materials Conference, 2018* (210049 2018). DOI: 10.2514/6.2018-2243. URL: https://arc.aiaa.org/doi/10.2514/6.2018-2243.

[11] Wenbin Yu. "Structure genome: Fill the gap between materials genome and structural analysis". In: *56th AIAA/ASCE/AHS/ASC Structures, Structural Dynamics, and Materials Conference* (2015). DOI: 10.2514/6.2015-0201. URL: https://arc.aiaa.org/doi/10.2514/6.2015-0201.

[12] Francesco S. Liguori et al. "An isogeometric framework for the optimal design of variable stiffness shells undergoing large deformations". In: *International Journal of Solids and Structures* 210-211 (Feb. 2021), pp. 18–34. ISSN: 0020-7683. DOI: 10.1016/J.IJSOLSTR.2020.11.003.

[13] Luan C. Trinh et al. "A mixed inverse differential quadrature method for static analysis of constant- and variable-stiffness laminated beams based on Hellinger-Reissner mixed variational formulation". In: *International Journal of Solids and Structures* 210-211 (Feb. 2021), pp. 66–87. ISSN: 0020-7683. DOI: 10.1016/J.IJSOLSTR.2020.11.019.

[14] R. M.J. Groh and P. M. Weaver. "A computationally efficient 2D model for inherently equilibrated 3D stress predictions in heterogeneous laminated plates. Part II: Model validation". In: *Composite Structures* 156 (Nov. 2016), pp. 186–217. ISSN: 0263-8223. DOI: 10.1016/J.COMPSTRUCT.2015.11.077.

[15] Saleh Yazdani and Pedro Ribeiro. "Geometrically non-linear static analysis of unsymmetric composite plates with curvilinear fibres: p-version layerwise approach". In: *Composite Structures* 118 (1 Dec. 2014), pp. 74–85. ISSN: 0263-8223. DOI: 10.1016/J.COMPSTRUCT.2014.07.007.

[16] Yufei Long, and Wenbin Yu. "Modelling of variable stiffness plates based on mechanics of structure genome". In: *Proceedings of the American Society for Composites: Thirty-First Technical Conference* 0 (0 2016). URL: http://dpi-proceedings.com/index.php/asc31/article/view/3277.

[17] Khizar Rouf, Xin Liu, and Wenbin Yu. "Multiscale structural analysis of textile composites using mechanics of structure genome". In: *International Journal of Solids and Structures* 136-137 (Apr. 2018), pp. 89–102. ISSN: 0020-7683. DOI: 10.1016/J.IJSOLSTR.2017.12.005.

[18] Xin Liu et al. "A unified approach for thermoelastic constitutive modeling of composite structures". In: *Composites Part B: Engineering* 172 (Sept. 2019), pp. 649–659. ISSN: 1359-8368. DOI: 10.1016/J.COMPOSITESB.2019.05.083.

[19] Fei Tao et al. "Multiscale analysis of multilayer printed circuit board using mechanics of structure genome". In: *Mechanics of Advanced Materials and Structures* 28 (8 2021), pp. 774–783. ISSN: 15376532. DOI: 10.1080/15376494.2019.1596335.

[20] Yufei Long et al. "Multiscale simulation of deployable composite structures". In: *AIAA Scitech 2021 Forum* (2021), pp. 1–21. DOI: 10.2514/6.2021-0199.

[21] Yufei Long et al. "Mechanics of Structure Genome-Based Nonlinear Shell Analysis". In: *AIAA Science and Technology Forum and Exposition, AIAA SciTech Forum 2022* (2022). DOI: 10.2514/6.2022-1119. URL: https://arc.aiaa.org/doi/10.2514/6.2022-1119.

[22] Wenbin Yu. "Mechanics of Materials and Structures A unified theory for constitutive modeling of composites". In: *Journal of mechanics of materials and structures* 11 (4 2016). DOI: 10.2140/jomms.2016.11.379. URL: https://cdmhub.org/resources/scstandard.

[23] Brian M Adams et al. *Dakota, A Multilevel Parallel Object-Oriented Framework for Design Optimization, Parameter Estimation, Uncertainty Quantification, and Sensitivity Analysis: Version 6.6 Theory Manual*.

[24] Adriana W. Blom, Patrick B. Stickler, and Zafer Gürdal. "Optimization of a composite cylinder under bending by tailoring stiffness properties in circumferential direction". In: *Composites Part B: Engineering* 41 (2 Mar. 2010), pp. 157–165. ISSN: 1359-8368. DOI: 10.1016/J.COMPOSITESB.2009.10.004.